



HAL
open science

Geometrical Calibration of the High Speed Robot Par4 Using a Laser Tracker

David Corbel, Olivier Company, Vincent Nabat, Patrick Maurine

► **To cite this version:**

David Corbel, Olivier Company, Vincent Nabat, Patrick Maurine. Geometrical Calibration of the High Speed Robot Par4 Using a Laser Tracker. MMAR'06: 12th International Conference on Methods and Models in Automation and Robotics, Aug 2006, Miedzyzdroje, Poland, Poland. pp.687-692. lirmm-00105708

HAL Id: lirmm-00105708

<https://hal-lirmm.ccsd.cnrs.fr/lirmm-00105708v1>

Submitted on 12 Oct 2006

HAL is a multi-disciplinary open access archive for the deposit and dissemination of scientific research documents, whether they are published or not. The documents may come from teaching and research institutions in France or abroad, or from public or private research centers.

L'archive ouverte pluridisciplinaire **HAL**, est destinée au dépôt et à la diffusion de documents scientifiques de niveau recherche, publiés ou non, émanant des établissements d'enseignement et de recherche français ou étrangers, des laboratoires publics ou privés.

Geometrical Calibration of the High Speed Robot Par4 using a Laser Tracker

David Corbel, Olivier Company, Vincent Nabat and Patrick Maurine

Abstract—This paper presents the geometrical calibration of the four-degree-of-freedom parallel manipulator Par4 using a laser tracker. After a brief presentation of Par4 and the measuring system, a simple inverse geometrical model suitable for robot control is derived. This model includes a minimal number of parameters thanks to the contraction of the traveling plate (end-effector) in a simple bar. Then, a calibration method based on distance measurement is explained and the simulation results are presented. Finally, the experimental results illustrate the benefits of the calibration.

I. INTRODUCTION

Nowadays, Parallel Kinematic Mechanisms (PKM) are still not used as often as serial ones. However, since the first parallel mechanism attributed to Gough [1], many others have been developed. In spite of recent research on the use of these mechanisms for machine tools, their main industrial application is packaging. Moreover, the most common parallel robot in industry is Delta robot, developed by Clavel at EPFL [2], whose main application is pick-and-place. This kind of task requires Scara motions ¹ (four degree-of-freedom (*dof*)). From the Delta mechanism and the concept of the articulated traveling plate, new architectures have been introduced: H4 [4], I4L [5], I4R [6] and finally Par4 [7].

This paper presents the calibration of this last mechanism. Indeed, robots are controlled with a model based on their nominal geometrical parameters. However, during the manufacturing and the assembly of robot elements, dimensioning errors appear between the real and nominal geometries. These errors cause positioning and orientating errors of the end-effector. In this context, geometrical calibration, which consists in an estimation of the real geometrical parameters, improves the accuracy of robots. Intensive research works have already been done on this subject [8] [9] [10] [11]. We can note that non-geometrical parameters also influence accuracy of robots like gear backlashes, static and dynamic elastic deformations [12] [13] [14] [15] [16]. However, this influence can generally be neglected in comparison with geometrical parameters. So, this paper only focuses on the identification of these last parameters.

Manuscript received March 27, 2006.

D. Corbel and O. Company are with the Laboratory of Computer Science, Robotics, and Microelectronics (LIRMM in French), 34392 Montpellier, France corbel@lirmm.fr company@lirmm.fr

V. Nabat is with the Fundación FATRONIK, E-20009 San Sebastián, Spain vnabat@fatronik.com

P. Maurine is with the Laboratory of Civil Engineering and Mechanical Engineering, National Institute for Applied Sciences (INSA), 35043 Rennes, France patrick.maurine@insa-rennes.fr

¹Motions produced by a Scara robot [3].

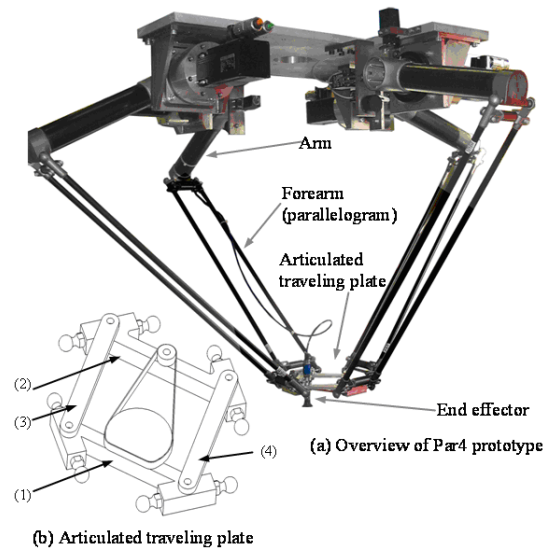


Fig. 1. Prototype of Par4

This paper presents the geometrical calibration of the four *dof* parallel manipulator Par4. This parallel manipulator belongs to the same family as H4 and I4 architectures which have already been calibrated by vision [17] [18]. In the following part, we recall the description of Par4 and we introduce the measurement system. In a second part, the geometrical and identification error models for the calibration are developed. Then, the calibration method is detailed and the simulation results are presented before a conclusion is reached with the experimental results.

II. DESCRIPTION OF PAR4 AND LASER TRACKER

A. Description of Par4

Par4 is a four *dof* robot dedicated to pick-and-place manipulations like Delta robot (three translations, one rotation). Its architecture is almost similar to that of H4 and I4 from which it derives. Only the traveling plate is different. Built like a variable parallelogram, the articulated traveling plate produces, via an amplification system, a rotational motion about vertical axis (see (b) in Fig. 1). The natural rotation of the traveling plate lets to obtain a quarter of turn ($\pm \frac{\pi}{4}$) whereas the amplification system allows to obtain a complete turn ($\pm \pi$). The kinematic modeling of Par4 is similar to the H4 one presented in [4]. Nevertheless, a minimal model has been developed for the calibration and it is presented in the following part.

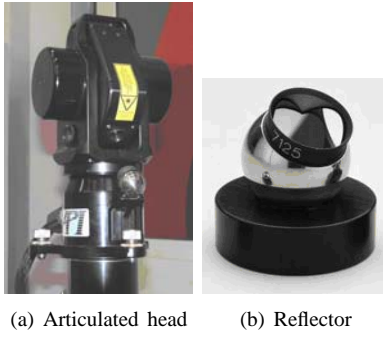


Fig. 2. Laser Tracker



Fig. 3. Corner cube on the traveling plate

B. Description of a laser tracker

The system of measurement used to calibrate the robot Par4 is a laser tracker, a fast and accurate three-dimensional Coordinate Measuring Machine (absolute accuracy: about $15 \mu m$). It is composed of an interferometric laser oriented along two directions by two motorized perpendicular rotation axes (see (a) in Fig. 2). The measured point is materialized by a reflector (see (b) in Fig. 2). The Cartesian coordinates of the measured point are obtained from the spherical coordinates given by the distance measured by the interferometer and the two angles of actuators.

The reflector (so-called corner cube) is realized by three mirrors included in a sphere. These mirrors create a corner cube which is located precisely at the center of the sphere. This reflector can be located via a magnetic support anywhere as long as the laser beam is not cut by an obstacle. In our case, the reflector is located on the Par4 traveling plate as shown in Fig. 3.

III. MODELING

A. Inverse Kinematic Model

In this part, the Inverse Kinematic Model used for the control of Par4 will be explained.

First of all, Fig. 4 illustrates the parametrization of the traveling plate. Points B_i represent the centers of the joints which link the forearms together with the traveling plate. Points C_i are the centers of the revolute joints located between the two main parts (see (1, 2) in Fig. 4) and two rods (see (3, 4) in Fig. 4). In order to optimize the number of parameters, the geometry of the traveling plate can be simplified (see (5) in Fig. 4). This simplification does not change the mechanism kinematics but avoids to take into

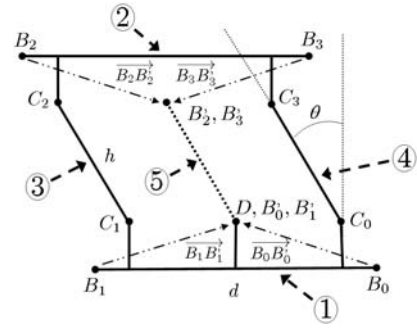


Fig. 4. Simplification of the traveling plate

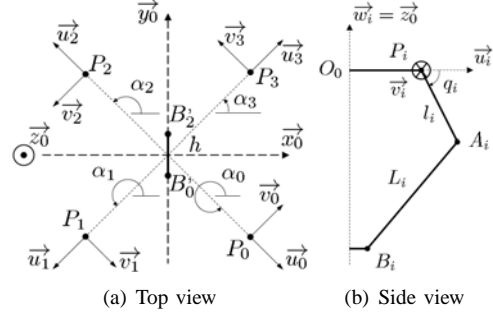


Fig. 5. Par4 geometrical parameters

account the geometrical parametrization of the traveling plate [19]. The translation of vector $B_i B'_i$ applied to the traveling plate must be applied to the positions of the motors too. These choices let to an optimal set of parameters that are all identifiable.

Moreover, the parallelograms of the forearms are considered as perfect. They are modeled as simple bars which are linked, in their first extremity, to the arms by universal joints and, in their second extremity, to the traveling plate by spherical joints.

In order to derive the model of the mechanism, the following frames have been defined (Fig. 5):

- $R_0(O_0, \vec{x}_0, \vec{y}_0, \vec{z}_0)$: the frame located on the base, \vec{x}_0 is along the side of the main part (see (1) in Fig. 4), \vec{z}_0 is normal to the plane motion of the traveling plate, \vec{y}_0 is normal to \vec{x}_0 and \vec{z}_0 .
- $R_{P_i}(P_i, \vec{u}_i, \vec{v}_i, \vec{w}_i)$: the frame located on the centers of the actuated joints P_i , \vec{w}_i is along \vec{z}_0 , \vec{v}_i represent the rotation axis of the motors, \vec{u}_i is normal to \vec{v}_i and \vec{w}_i .

The geometrical parameters used to derive the Par4 inverse position relationship are presented in Fig. 5. One can note ($i \in [0, 3]$):

- $x_{p_i}, y_{p_i}, z_{p_i}$: the positions of the motor centers P_i in R_0 ,
- α_i : the orientation of motor axes around \vec{z}_0 ,
- q_i : the positions of the actuators,
- l_i : the length of arms,
- L_i : the length of forearms,
- h : the length of the parallelogram of the traveling plate.

Vector \mathbf{K} including the twenty nine geometrical parameters is defined as follows:

$$\mathbf{K} = [x_{p_0}, y_{p_0}, z_{p_0}, \alpha_0, q_0, l_0, L_0, x_{p_1}, y_{p_1}, z_{p_1}, \alpha_1, q_1, l_1, L_1,$$

$$x_{p_2}, y_{p_2}, z_{p_2}, \alpha_2, q_2, l_2, L_2, x_{p_3}, y_{p_3}, z_{p_3}, \alpha_3, q_3, l_3, L_3, h]^T \quad (1)$$

Their nominal values will be defined by vector \mathbf{K}_0 according to the following relation:

$$\mathbf{K} = \mathbf{K}_0 + \delta\mathbf{K} \quad (2)$$

The controlled point B'_0 (or B'_1) position and the traveling plate orientation are given by $\mathbf{x} = [X, Y, Z, \theta]^t$ in R_0 . θ represents the natural rotation angle of the traveling plate i.e. without the amplification system. The positions of the actuators are given by $\mathbf{q} = [q_0, q_1, q_2, q_3]^t$.

The position relationships between the controlled point \mathbf{x} and the actuated joints values \mathbf{q} , are obtained from closing loops equations:

$$\|\overrightarrow{A_i B_i}\|^2 = l_i^2 \quad (3)$$

Points P_i are given by the matrix:

$$\mathbf{P} = \begin{bmatrix} x_{P_0} & x_{P_1} & x_{P_2} & x_{P_3} \\ y_{P_0} & y_{P_1} & y_{P_2} & y_{P_3} \\ z_{P_0} & z_{P_1} & z_{P_2} & z_{P_3} \end{bmatrix} \quad (4)$$

The column i represents the coordinates of points P_i . This convention is used here for points but also for vectors.

Vectors \overrightarrow{u}_i and \overrightarrow{v}_i of frames R_{P_i} are defined by the matrices:

$$\mathbf{U} = \begin{bmatrix} \cos\alpha_0 & \cos\alpha_1 & \cos\alpha_2 & \cos\alpha_3 \\ \sin\alpha_0 & \sin\alpha_1 & \sin\alpha_2 & \sin\alpha_3 \\ 0 & 0 & 0 & 0 \end{bmatrix} \quad (5)$$

$$\mathbf{V} = \begin{bmatrix} -\sin\alpha_0 & -\sin\alpha_1 & -\sin\alpha_2 & -\sin\alpha_3 \\ \cos\alpha_0 & \cos\alpha_1 & \cos\alpha_2 & \cos\alpha_3 \\ 0 & 0 & 0 & 0 \end{bmatrix} \quad (6)$$

Points A_i represent the centers of joints which link the arms together with the forearms. They can be defined in frames R_{P_i} as follows:

$$\mathbf{A} = \begin{bmatrix} l_0 \cos q_0 & l_1 \cos q_1 & l_2 \cos q_2 & l_3 \cos q_3 \\ 0 & 0 & 0 & 0 \\ -l_0 \sin q_0 & -l_1 \sin q_1 & -l_2 \sin q_2 & -l_3 \sin q_3 \end{bmatrix} \quad (7)$$

So, points A_i expressed in frame R_0 are given by:

$$\mathbf{A} = \mathbf{P} + \begin{bmatrix} l_0 \cos q_0 \cos \alpha_0 & l_1 \cos q_1 \cos \alpha_1 \\ l_0 \cos q_0 \sin \alpha_0 & l_1 \cos q_1 \sin \alpha_1 \\ -l_0 \sin q_0 & -l_1 \sin q_1 \\ l_2 \cos q_2 \cos \alpha_2 & l_3 \cos q_3 \cos \alpha_3 \\ l_2 \cos q_2 \sin \alpha_2 & l_3 \cos q_3 \sin \alpha_3 \\ -l_2 \sin q_2 & -l_3 \sin q_3 \end{bmatrix} \quad (8)$$

Points B'_i can be expressed in R_0 as follows:

$$\mathbf{B}' = \begin{bmatrix} X & X & X - h \sin \theta & X - h \sin \theta \\ Y & Y & Y + h \cos \theta & Y + h \cos \theta \\ Z & Z & Z & Z \end{bmatrix} \quad (9)$$

It is now possible to use the hypothesis (3). The system of equation can be written as follows:

$$I_i \sin q_i + J_i \cos q_i + K_i = 0 \quad (10)$$

where

$$I_i = -2l(\overrightarrow{P_i B_i} \cdot \overrightarrow{x_0} \cos \alpha_i + \overrightarrow{P_i B_i} \cdot \overrightarrow{y_0} \sin \alpha_i) \quad (11)$$

$$J_i = 2l \overrightarrow{P_i B_i} \cdot \overrightarrow{x_0} \quad (12)$$

$$K_i = L^2 - l^2 - \|\overrightarrow{P_i B_i}\|^2 \quad (13)$$

Using the variable change $t_i = \tan(\frac{q_i}{2})$, we obtain the polynomial system:

$$(I_i - J_i)t_i^2 + 2I_i t_i + (J_i + K_i) = 0 \quad (14)$$

We deduce

$$\Delta_i = I_i^2 - K_i^2 + J_i^2 \quad (15)$$

If all Δ_i are positive, the traveling plate position is accessible, and actuated joint unknowns are given by:

$$q_i = 2 \operatorname{atan} \left(\frac{-I_i \pm \sqrt{\Delta_i}}{K_i - J_i} \right) \quad (16)$$

A quick geometrical study permits to eliminate one of the two solutions for each variable. Indeed, q_i is obtained using:

$$q_i = 2 \operatorname{atan} \left(\frac{-I_i - \sqrt{\Delta_i}}{K_i - J_i} \right) \quad (17)$$

B. Forward Kinematic Model

As described in [19], the analytic calculation of direct position relationship for this type of robot is impossible. But, in this case, it is possible to use Newton iterative algorithm. This iterative algorithm permits to obtain approached solution of absolute coordinates by using Jacobian Matrix \mathbf{J} (presented in [7]) and the inverse position relationship:

$$\mathbf{x}_{n+1} = \mathbf{x}_n + \mathbf{J}(\mathbf{x}_n, \mathbf{q}_n) \cdot [\mathbf{q}_d - \mathbf{q}_n] \quad (18)$$

IV. CALIBRATION

A. Experimental Set-up

Fig. 6 shows the experimental set-up. The laser tracker is installed at about 2.5 meters to ensure that the Par4 workspace is within the volume of measurement of the laser tracker. The reflector is stuck on the traveling plate via a magnetic support as shown on Fig. 3. The laser tracker allows to take a lot of measurements in the whole Par4 workspace. **The calibration method, explained below, is independent of the measuring frame, so the location of laser tracker in relation with the robot is not important [20].** In an industrial context, this is very interesting since the set-up of the measurement system is fast and easy.

B. Calibration Method

First of all, the calibration method is based on distance measurement rather than absolute position measurement. Indeed distances are independent of any frame, so the laser tracker can be located anywhere like explained previously. Moreover, this method allows to avoid errors which could arise from the transformation between the laser tracker frame and the robot frame. Calibration methods based on distance measurements are presented in [20] or [21], but these methods rely on an artefact. So, a little part of the

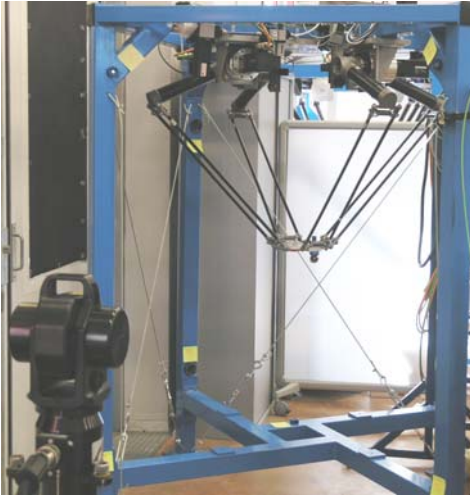


Fig. 6. Experimental set-up

workspace is used whereas, with the laser tracker, we have measurements in the whole workspace of the robot and thus we have a better signature of the robot parameters.

The calibration method consists in minimizing the quadratic errors between N nominal distances \mathbf{D}^n and N real distances \mathbf{D}^r . These distances are calculated from N couples of points defined in advance. For correct calibration, N must be larger than the number of identified parameters. Estimation of the errors on the geometrical parameters $\delta\mathbf{K}$ is obtained from a least square minimization of an error function as described below:

$$\min_{\delta\mathbf{K}} \sum_{i=1}^N (D_i^n - D_i^r)^2 \quad (19)$$

This non-linear optimization is achieved by using the Levenberg-Marquardt algorithm. Then, we use (2) to estimate the real geometrical parameters.

C. Hypothesis for the Calibration

Several hypotheses on Par4 geometry are made in order to simplify the model:

- (i) the traveling plate is considered always parallel to a plane whose normal is \vec{z}_0 ,
- (ii) the motor axes are supposed to be perpendicular to \vec{z}_0 ,
- (iii) they are supposed to be perpendicular between them ($\alpha_i = \frac{\pi}{4} + (3-i)\frac{\pi}{2}$),
- (iv) the forearm parallelograms are assumed perfect (Fig. 1).

The hypothesis (ii) is conveyed by the following equation:

$$\vec{v}_i \cdot \vec{z}_0 = 0 \quad (20)$$

The hypothesis (iii) is expressed by this equation ($j \in [0, 3]$):

$$\vec{v}_i \cdot \vec{v}_j = 0 \quad i \neq j \quad (21)$$

Concerning assumption (iv), a method is presented in [22] which makes it possible to compensate for the position errors

TABLE I
NOMINAL GEOMETRICAL VALUES AND THEIR SIMULATED ERRORS

Parameter nominal values	Error values	Unit
$q_i \in [-45^\circ, 45^\circ] \quad i \in [0, 3]$	$\delta q_0 = -0.1, \delta q_1 = 0.2,$ $\delta q_2 = -0.3, \delta q_3 = 0.1$	deg
$x_{p_1} = x_{p_2} = 172.5$ $x_{p_0} = x_{p_3} = -172.5$	$\delta x_{p_0} = 0, \delta x_{p_1} = -1,$ $\delta x_{p_2} = -2, \delta x_{p_3} = -2$	mm
$y_{p_0} = y_{p_1} = -222.5$ $y_{p_2} = y_{p_3} = 222.5$	$\delta y_{p_0} = 0, \delta y_{p_1} = -3,$ $\delta y_{p_2} = -3, \delta y_{p_3} = 1$	mm
$z_{p_0} = z_{p_1} = z_{p_2} = z_{p_3} = 0$	$\delta z_{p_0} = 0, \delta z_{p_1} = 2,$ $\delta z_{p_2} = -1, \delta z_{p_3} = 3$	mm
$l_0 = l_1 = l_2 = l_3 = 350$	$\delta l_0 = 2, \delta l_1 = 3,$ $\delta l_2 = 3, \delta l_3 = -1$	mm
$L_0 = L_1 = L_2 = L_3 = 350$	$\delta L_0 = -1, \delta L_1 = 1,$ $\delta L_2 = 1, \delta L_3 = -3$	mm
$h = 100$	$\delta h = 1$	mm

of the controlled point due to the geometrical errors of the forearms parallelograms.

Finally, we assume that point P_0 is well positioned in R_0 ($\delta x_0 = \delta y_0 = \delta z_0 = 0$). Point P_0 could be the origin of the frame R_0 , but to keep the symmetry, O_0 is located in the theoretic barycenter of points P_i .

D. Simulation Results

This part presents the simulation validation of the calibration method and the parameter choice. This simulation consists in taking a random set of values of geometrical errors and to identify it with the calibration method (see TABLE I).

The simulated, measured points are taken near the boundary of the workspace to get the best signature of the robot parameters ($N = 60$). For each configuration, measurement of complete position $[X, Y, Z]$ of the controlled point B'_0 is available. The traveling plate orientation is not measured. Moreover, a Gaussian measuring noise with standard deviation of $\frac{0.015}{\sqrt{3}}$ mm is defined on each coordinates.

Fig. 7 shows the improvement obtained with the estimation of the geometrical parameters. Before calibration (blue points), the maximum distance errors ($D_i^n - D_i^r$) reach about 10 mm. After calibration (red cross), these errors are almost null ($< 10 \mu m$). The parameters are identified with an accuracy of 0.05 mm and 0.002° . So, this simulation allows to verify that the potential noise of measurement introduced by the laser tracker does not skew the estimation of the parameters.

It should be also noted that the repeatability of the robot can intervene in a negative way in the identification of the geometrical parameters. Indeed, the repeatability value can be considered as an uncertainty of measurement. So, a simulation with a uniformly distributed uncertainty of $\frac{0.4}{\sqrt{3}}$ mm on each coordinates is made. The maximum distance errors reach about 0.3 mm, and the errors on the estimation of the parameters are about 1mm and 0.1° . So, the calibration algorithm allows to estimate parameters which improve the

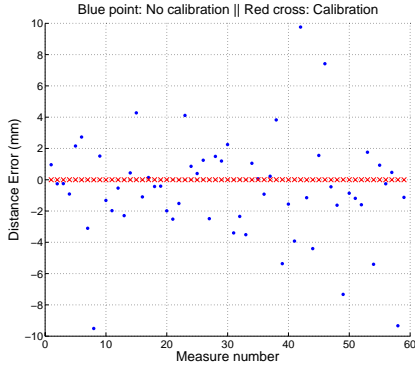


Fig. 7. Error on the distance between two measured points

robot accuracy even if these parameters are not the real geometrical parameters.

E. Experimental Results

1) *Repeatability Test:* Before calibration, the repeatability of our Par4 prototype has been tested in order to know perfectly the capabilities of the robot. The performed test is a multi-directional repeatability test at the center of the workspace. This test consists in reaching several times (in our case 28 times), the same point following different trajectories. The preliminary results show that the radius of the position uncertainty sphere due to the repeatability of Par4 is about 0.4 mm. So, it is obvious that the absolute accuracy of the robot cannot be better than 0.4 mm as shown by the simulation. Moreover, the estimated parameters obtained by the optimization will not be the real parameters.

Several effects can influence the Par4 repeatability: the backlashes in the gear reducer, the friction in the spherical joints. For example, a backlash of 1' on the actuated joints induced a motion of 0.1 mm at the extremity of the arms.

2) *Parameter Identification:* The experimental results presented in this part have been obtained thanks to the experimental device shown in Fig. 3 and Fig. 6. 60 real distances have been calculated corresponding to 120 measured points. The nominal distances have been calculated with the forward kinematic relationships from the measured actuated joint values and compared with the real distances (see blue points in Fig. 8).

Then, the identification is achieved thanks to the Levenberg-Marquardt algorithm as explained previously. The results obtained with the calibration methods are given in TABLE II.

The errors on the geometrical parameters are large compared to the values of manufacturing and assembly tolerances which are, at least, lower than 1 mm. These error values do not correspond to a physical reality but they make it possible to improve the precision of the robot like one shown simulations.

3) *Compensation and Validation:* The geometrical parameters are updated with the estimated errors (see (2)) and introduced in the robot command. Then, new series of measurements are collected with the laser tracker to see an

TABLE II
ESTIMATED ERRORS ON THE GEOMETRICAL PARAMETERS

δq_0 (deg)	δq_1 (deg)	δq_2 (deg)	δq_3 (deg)	δx_{p_1} (mm)	δx_{p_2} (mm)	δx_{p_3} (mm)	δy_{p_1} (mm)
-4.04	-4.84	-4.54	-3.86	-5.00	2.78	-0.72	5.76
δy_{p_2} (mm)	δy_{p_3} (mm)	δz_{p_1} (mm)	δz_{p_2} (mm)	δz_{p_3} (mm)	δl_0 (mm)	δl_1 (mm)	δl_2 (mm)
-7.23	0.13	0.26	-1.25	-1.45	-4.21	-1.37	-7.71
δl_3 (mm)	δL_0 (mm)	δL_1 (mm)	δL_2 (mm)	δL_3 (mm)	δh (mm)		
2.46	1.26	1.41	-1.61	4.04	-1.55		

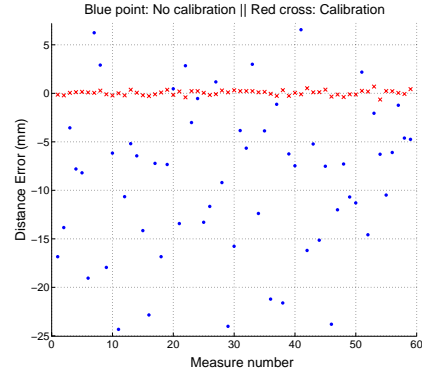


Fig. 8. Error on the distance between two measured points

improvement in the accuracy of the robot. Fig. 8 shows the improvement due to the calibration. Before calibration (blue points), there are errors superior to 20 mm. After calibration (red cross), the errors are about 0.6 mm.

A first validation consists in fixing the position of the traveling plate and carrying out only one rotation from $\theta = -45^\circ$ to $\theta = 45^\circ$. Before calibration, the traveling plate moves of approximately 2 mm during rotation, and after calibration, it moves only of 0.2 mm.

A second validation consists in verifying the straightness of a software defined line. The chosen lines are along the axes \vec{x}_0 , \vec{y}_0 and \vec{z}_0 . The length of these lines are respectively 800 mm, 800 mm and 500 mm and they pass through the center of the robot workspace. TABLE III shows the improvement of the straightness obtained with the calibration.

The improvement in straightness along \vec{z}_0 is not large compared to the other axes. This is explained by the fact that the initial straightness along this axis was already low (close to the repeatability value).

A third validation consists in verifying the absolute accuracy of Par4 in the laser tracker frame R_L . For this validation, a transformation between R_L and R_0 can be identified in order to determine the absolute accuracy of Par4.

The position of a point 0P , defined in R_0 , can be defined in the frame R_L by (\mathbf{R} denote the homogeneous matrix of the rotation) :

$${}^L\mathbf{P} = {}^L\mathbf{T}_0.{}^0\mathbf{P} \quad (22)$$

TABLE III
STRAIGHTNESS BEFORE AND AFTER CALIBRATION

	Straightness along \vec{x}_0 (mm)	Straightness along \vec{y}_0 (mm)	Straightness along \vec{z}_0 (mm)
Before calibration	5.48	5.62	0.91
After calibration	0.20	0.61	0.55
Gain	96%	89%	60%

TABLE IV
RESULTS ON VALIDATION POINTS

	Mean error on distances (mm)	Max error on distances (mm)
Before calibration	7.3	15.2
After calibration	0.4	1.2
Gain	95%	92%

where

$${}^L\mathbf{T}_0 = \mathbf{R}(\vec{z}, \varphi) \cdot \mathbf{R}(\vec{y}, \gamma) \cdot \mathbf{R}(\vec{x}, \psi) \cdot {}^L\mathbf{O}_0 \quad (23)$$

$${}^L\mathbf{O}_0 = [O_{0x}, O_{0y}, O_{0z}]^t \quad (24)$$

The parameters φ , γ , ψ , O_{0x} , O_{0y} and O_{0z} are estimated from a least square minimization as described below:

$$\min_{\varphi, \gamma, \psi, O_{0x}, O_{0y}, O_{0z}} \sum_{i=1}^N ((X_i^n - X_i^r)^2 + (Y_i^n - Y_i^r)^2 + (Z_i^n - Z_i^r)^2) \quad (25)$$

X^n , Y^n , Z^n are the nominal values of the coordinates of controlled point in R_L and X^r , Y^r , Z^r are the real values of the coordinates of the controlled point in R_L . Then, it is possible to characterize the absolute accuracy of the robot in the laser tracker frame. Results are presented in TABLE IV.

TABLE IV shows that the absolute accuracy is improved, and becomes close to the repeatability value.

V. CONCLUSIONS AND FURTHER WORKS

In this paper, we have presented the geometrical calibration of the pick-and-place robot Par4 based on a minimization of an error function. The measuring system used to measure the distances required for the calibration was a laser tracker. After the presentation of the Par4 geometrical model, the calibration method was explained. Based on distance measurements, it allows to calibrate the robot without defining any reference frame. This calibration made it possible to improve the accuracy of the robot of about 90%. The influence of the repeatability on the calibration was also highlighted and further work will concern the study of this phenomenon.

REFERENCES

[1] V. E. Gough, "Contribution to Discussion of Papers on Research in Automotive Stability, Control and Tyre Performance," in *Proc. Auto Div.*, Institute of mechanical engineering, 1956-1957.
[2] R. Clavel, "Conception d'un Robot Parallèle Rapide à 4 Degrés de Liberté," Ph.D. dissertation, EPFL, Lausanne, Switzerland, 1991.

[3] N. Furuya, K. Soma, E. Chin, and Makino, "Research and Development of Selective Compliance Assembly Robot Arm," in *Hardware and Software of SCARA Controller*, J. Japan Soc. Precision Eng./Seimitsu Kogaku Kaishi, vol. 49, no. 7, 1983, pp. 835-841.
[4] F. Pierrot and O. Company, "H4: a New Family of 4-dof Parallel Robots," in *IEEE/ASME International Conference on Advanced Intelligent Mechatronics (AIM'99)*, Atlanta, Georgia, USA, September 1999, pp. 508-513.
[5] S. Krut, O. Company, M. Benoit, H. Ota, and F. Pierrot, "I4: A New Parallel Mechanism for Scara Motions," in *IEEE International Conference on Robotics and Automation (ICRA'03)*, Taipei, Taiwan, September 2003.
[6] S. Krut, V. Nabat, O. Company, and F. Pierrot, "A High Speed Robot for Scara Motions," in *IEEE International Conference on Robotics and Automation (ICRA'04)*, New Orleans, USA, April 26-May 1 2004.
[7] V. Nabat, O. Company, S. Krut, M. Rodriguez, and F. Pierrot, "Par4: Very High Speed Parallel Robot for Pick-and-Place," in *Proc. IEEE International Conference on Intelligent Robots and Systems (IROS'05)*, Edmonton, Alberta, Canada, August 2005.
[8] P. Vischer and R. Clavel, "Kinematic Calibration of the Parallel Delta Robot," in *Robotica*, vol. 16(2), March-April 1998, pp. 207-218.
[9] S. Besnard, "Étalonnage Géométrique de Robots Série et Parallèles," Ph.D. dissertation, École Centrale de Nantes, Nantes, France, 2000.
[10] D. Daney, "Étalonnage Géométrique des Robots Parallèles," Ph.D. dissertation, Université de Nice - Sophia Antipolis, Nice, France, 2000.
[11] K. Grossman, B. Wunderlich, and S. Szatmari, "Progress in Accuracy and Calibration of Parallel Kinematics," in *Proc. Parallel Kinematics Seminar (PKS'04)*, Chemnitz, Germany, April 2004, pp. 49-68.
[12] C. M. Gosselin and D. Zang, "Stiffness Analysis of Parallel Mechanisms using a Lumped Model," in *International Journal of Robotics and Automation*, vol. 17, no. 1, 2002, pp. 17-27.
[13] G. Ecorchard and P. Maurine, "Self-calibration of Delta Parallel Robots with Elastic Deformation Compensation," in *Proc. IEEE International Conference on Intelligent Robots and Systems (IROS'05)*, Edmonton, Alberta, Canada, August 2005.
[14] G. Ecorchard, R. Neugebauer, and P. Maurine, "Self-calibration of a Redundantly Actuated Parallel Kinematic Machine Tool," in *Proc. Parallel Kinematics Seminar (PKS'06)*, Chemnitz, Germany, April 2006.
[15] D. Deblaise, X. Hernot, and P. Maurine, "A Systematic Analytical Method for PKM Stiffness Matrix Calculation," in *IEEE International Conference on Robotics and Automation (ICRA'06)*, Orlando, Florida, USA, May 2006.
[16] D. Deblaise and P. Maurine, "Analytical Modeling of PKM Stiffness based on Matrix Structural Analysis," in *Proc. Parallel Kinematics Seminar (PKS'06)*, Chemnitz, Germany, April 2006.
[17] P. Renaud, N. Andreff, F. Marquet, and P. Martinet, "Vision-based Kinematic Calibration of a H4 Parallel Mechanism," in *IEEE International Conference on Robotics and Automation (ICRA'03)*, Taipei, Taiwan, September 2003, pp. 1191-1196.
[18] P. Renaud, N. Andreff, F. Pierrot, and P. Martinet, "Combining End-effector and Legs Observation for Kinematic Calibration of Parallel Mechanisms," in *IEEE International Conference on Robotics and Automation (ICRA'04)*, News Orleans, USA, April 26-May 1 2004, pp. 4116-4121.
[19] O. Company, "Machines-outils Rapides à Structure Parallèle. Méthodologie de Conception, Applications et Nouveaux Concepts," Ph.D. dissertation, Université Montpellier II, Montpellier, France, 2000.
[20] C. Gong, J. Yuan, and J. Ni, "A Self-calibration Method for Robotic Measurement System," in *Journal of Manufacturing Science and Engineering*, vol. 122, 2000, pp. 174-181.
[21] D. Deblaise and P. Maurine, "Effective Geometrical Calibration of a Delta Parallel Robot used in Neurosurgery," in *Proc. IEEE International Conference on Intelligent Robots and Systems (IROS'05)*, Edmonton, Alberta, Canada, August 2005.
[22] L. Savoure, P. Maurine, D. Corbel, and S. Krut, "An Improved Method for the Geometrical Calibration of Parallelogram-based Parallel Robots," in *IEEE International Conference on Robotics and Automation (ICRA'06)*, Orlando, Florida, USA, May 2006.